Diagenesis of Palaeozoic-Mesozoic Tethys ocean carbonate succession-Oman mountains

Alham Al-langawi

PAAET - College of Basic Education, Dept. of Science, Kuwait,
P.O. Box: 23167 Safat,13092 Kuwait.

Corresponding author: ajharock2011@hotmail.com

Abstract

This paper studies the uppermost unit of the Kharus formation (Cambrian) and the Autochthonous Akhdar group (Permian-Triassic), which unconformably covers the pre-Permian strata. The petrographic, geochemical, and field observations indicate that the succession underwent different stages of dolomitization that produced rocks inheriting the original host rock textures and structures (fabric-preserving dolomitization) and rocks with complete obliteration of the pre-existing textures (fabric-destroying dolomitization). The Dolomites that retain the actual fabric of the limestone are indicators of the host rock mineralogy, i.e., whether it was made up of high Mg-calcite or aragonitic allochems, and indicate early dolomitization. The top part of the Kharus Formation consists of pervasively dolomitized units, whereas dolomites are belonging to the Autochthonous Akhdar group display variable degrees of structural and textural preservation. The evidence suggests very early dolomitization in a relatively short time interval for the Permian-Triassic carbonates. The preserved depositional features in the Permian-Triassic carbonates indicate deposition in shallow marine environments with variable energy levels. Seven facies are inferred: stromatolites, mudstones, wackestones, intraformational breccias, grainstones, and grain/packstones. Petrographic as well as field observations exclude evidence of evaporites within Palaeozoic-Mesozoic rocks. Five paragenetic phases are determined to explain the type of dolomitization and indicate the type and severity of diagenesis that affected the Palaeozoic-Mesozoic Tethys Ocean carbonates from the Oman Mountains.

Keywords: Akhdar group; kharus formation; oman mountains; palaeozoic-mesozoic dolomites; paragenetic phases

1. Introduction

The different diagenetic conditions the precursor rocks underwent are essential in producing various dolomites, including the evaporitic, replacement, and cement dolomites (McKenzie *et al*., 1980; Gunatilaka, 1987; Randazzo and Cook, 1987; Tucker, 2001). Differences in crystal habits, textures, and compositions of the fabric components of each dolomite type reflect differences in environments and time of formation, the mode of formation, and the nature of the original limestone (Mattes & Mountjoy, 1980; Gunatilaka, 1987; Dawson & Carozzi, 1993; Arenas *et al*. 1999; Zainal Abidian *et al*. 2017). Usually, fluctuation in sea level produces fluctuation in the position of the marine, meteoric, and mixing zones phreatic environments.

The shift in the phreatic zones is the main factor governing the type and extent of digenesis, hence the dolomitization that the host rocks experienced.

Most processes of diagenetic dolomitization require the dissolution of pre-existing carbonates and recrystallisation as dolomites, and most dolomites in the stratigraphic record are late diagenetic replacements (keeping in mind the known examples of primary dolomites in the geological record). These diagenetic processes can occur at the near-surface or depths within sedimentary basins, but the chemical and physical factors controlling the dolomitization in any environment will result in the development of various compositional and textural characteristics within the dolomites.

The major exposure of the pre-Permian-Triassic rocks can be found at the Saih Hatat window, with other smaller exposures at the Sahtan, Kharus, and Mistal windows (Figure 1). Shallow marine and terrestrial sediments of the Late Proterozoic to Early Palaeozoic age comprise the pre-Permian strata and are considered the oldest exposed rocks in the area (Glennie *et al.* 1974; Gealey 1977; Mann & Hanna 1990; Veerle & Cedric 2012). Mann & Hanna (1990) point out the thickness of the Kharus Formation is 180 m and is of Cambrian age. Mann and Hanna (1990) added that the older section of the Kharus Formation comprises laminated lime mudstones. In contrast, the younger section is a massive carbonate unit consisting of stromatolites, chert nodules, and oolitic limestones.
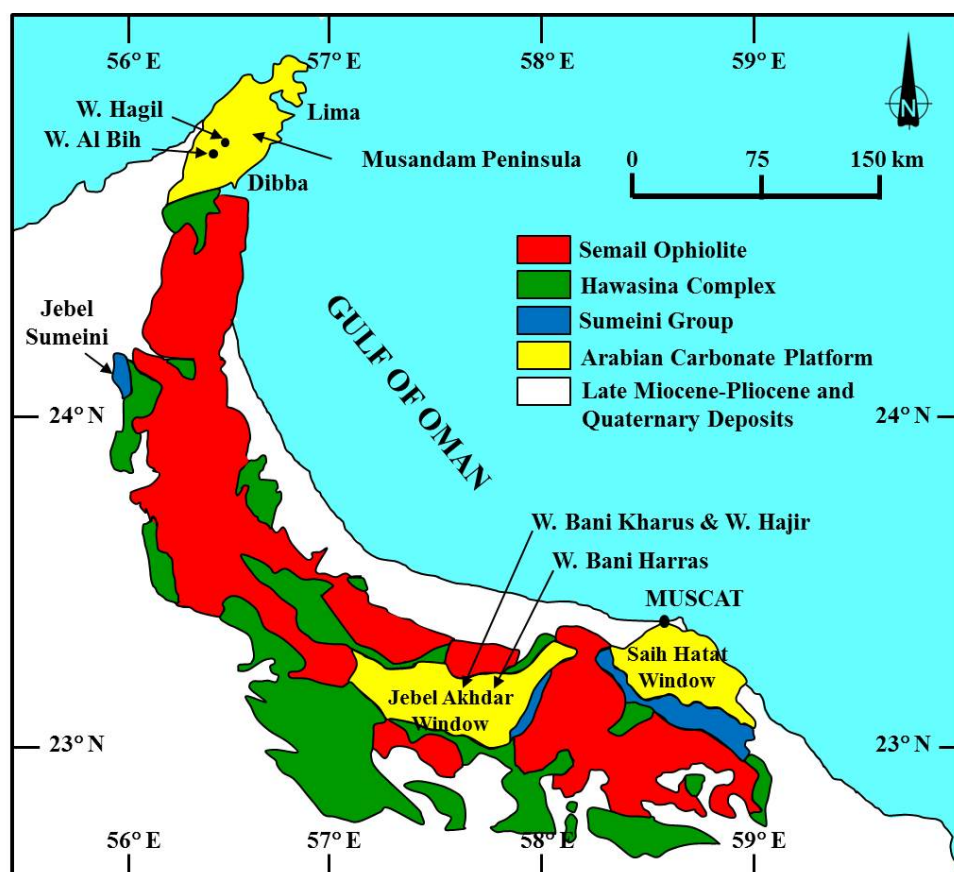
Fig. 1. Simplified geologic map showing the geology of the Oman Mountains and the locations of the studied areas.

Coleman 1981 indicated in his study that during the Cambrian-Pliocene, 5500 m thick shelf sediments were deposited across the Arabian Peninsula. The main factors attributed to this thick succession are climate and continuous subsidence (Murris 1980). During the Permian, a low supply of clastic materials reached the basin from the west (Arabian Shield), which later increased during the Early Triassic (Murris 1980).

Glennie *et al*. (1973, 1974, 1990) proposed the first thorough stratigraphy of the Oman Mountains. The Oman Mountain rocks were subdivided into five groups, as shown in (Figure 2).

The folded and imbricated pre-Permian rocks are unconformably covered by the autochthonous rocks (Wilson 1969, 1985; Glennie *et al*. 1973; Gealey 1977; Ricateau & Riche 1980; Searle & Graham 1982; Searle *et al*. 1983; Wilson 1985; Robertson *et al*. 1990). Glennie *et al*. (1973) segmented the shelf rocks into two main divisions. The first division is the Lower Palaeozoic carbonates and clastics, whereas Permian-Late Cretaceous shelf carbonates comprise the second unit. The Hajar Supergroup developed in shallow marine and supratidal environments displaying evidence of emergent-disconformity surfaces (Glennie *et al*. 1973, 1974). Glennie *et al*. (1973, 1974); Welland & Mitchell (1977); Baud & Richoz (2013); Khalaf & Al-Zamel (2018) named the lower part of the Hajar Supergroup (Mid-Upper Permian to Triassic) Akhdar Group with further subdivisions into Saiq and Mahil formations (Figure 2).
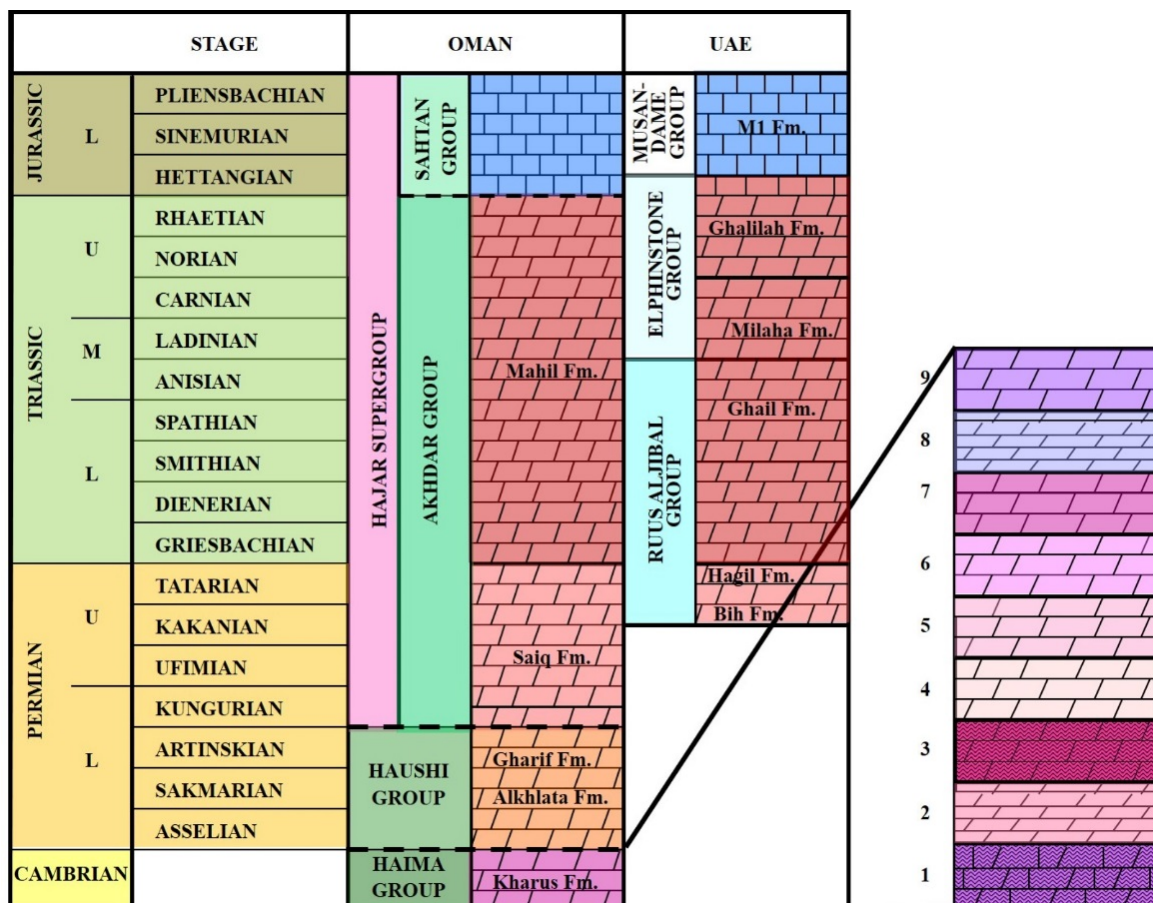
Fig. 2. Stratigraphy of the Oman Mountains and the Musandam Peninsula (Oman and the UAE).

This research aims to explain the diagenetic history of the Palaeozoic-Mesozoic Tethys Ocean carbonates from the Oman Mountains. In addition, to indicate the type and severity of diagenetic processes that affected the rocks, schematic paragenetic phases are determined for the different methods inferred from the petrographic and geochemical study. Al-langawi (2006) addresses the complete description of the Oman Mountains autochthonous formations of the Permian-Triassic age. It summarizes the petrographic and geochemical work done on these rocks. It shows the shift in the phreatic zones (meteoric and marine) that affected the shelf carbonates and resulted in various textures and fabrics. This research also clarifies the dolomitization mechanism for all the pre-Permian to Triassic rocks based on new geochemical and petrographic data. Correlating and merging data between the two studies yields a better perspective on diagenesis and dolomitization of the Palaeozoic-Mesozoic rocks from the Oman Mountains. The Cambrian Kharus Formation was not part of the research published in 2006.

2. Methodology

After careful examination of topographic and geologic maps and aerial photographs, a sampling of the Paleozoic-Mesozoic carbonates was carried out. Wadi Hijir, a tributary of Wadi Bani Kharus at Jabal Nakhal, is the best place to map and sample the 36 meters exposed section of The Kharus Formation. Jebel Akhdar, Wadi Al Bih, Wadi Hagil (Musandam Peninsula), and Jebel Sumeini are the best locations for mapping and sampling Permian-Triassic carbonates (Figure 1).

Uncovered thin sections were initially examined by staining with potassium ferricyanide and Alizarin Red-S for classification of calcite and dolomite content of the rocks (Adams *et al*. 1984), hence into limestones and dolomites. After staining, the second stage is the petrographic examination of the thin polished sections by the polarizing microscope, scanning electron microscopy (backscattered images), and cathodoluminescence microscope.

The thin polished sections' geochemical examination was conducted using an electron microprobe and semi-quantitative analysis by the scanning electron microscope (SEM). The Jeol-6400 (SEM) fitted with a Link Analytical Qualitative X-ray energy-dispersive spectrometer (EDS) was used for analyzing the thin polished sections. The chosen samples for X-ray diffraction are either whole-rock samples or separated dolomite crystals displaying crystal size and texture variations. An X-ray diffractometer (PW1730 Philips) fitted with a PW1050 goniometer was used for the qualitative examination. The samples were analyzed using a CAMECA CAMEBAX electron microprobe with a qualitative energy dispersive spectrometer, two-wavelength dispersive spectrometers (WDS), and a Link Analytical AN10/85S EDS system. The Zaf-4/FLS software was used for manually operated EDS analysis and software called "SPECTRA" for automated EDS or EDS plus WDS analysis. Element maps were created for chosen samples to display the major and trace element distributions and concentrations. The isotope analysis was carried out by using a VG Isogas SIRA12 mass spectrometer (SIRA= stable isotope ratio analyzer) at the Earth Science Department of Liverpool University. The temperature of the reaction was 50°C, and the phosphoric acid fractionation factor used was 1.01011. Whole-

rock samples or separated dolomite crystals displaying crystal size and texture variations were ground in preparation for isotope analysis.

3. Petrography

All the rocks from the top part of the Kharus Formation include crystalline dolomites, which are either coarse crystalline or thinly laminated and fine to medium crystalline, crosscut by various cemented veins of dolomites and calcites (Figure 3). The dolomitization of this section is pervasive, and no indication of previous texture or rock type is detected. The top 36 meters of the Kharus Formation consists of 9 units starting with microcrystalline lime-dolostone at the bottom, preceded by 8 dolomite units (Figure 2). All the units are intercalated with fractures, cemented by dolomite spars (some are rhombic), fine-coarse crystalline calcite, and iron oxides.

The exposed section at Wadi Hijir of the Kharus Formation starts with a one-meter-thick dark grey stromatolitic unit composed of cloudy microcrystalline calcite and dolomite. This older lime-dolostone unit contains wide and microcrystalline fractures cemented by dolomite spars. Next, a thinly laminated three-meter-thick dolomite unit with alternating light grey and light brown layers covers the first unit. The thin layers are either composed of microcrystalline or medium crystalline dolomite crystals. Finally, fractures crosscut the second unit and are cemented by calcite spars.
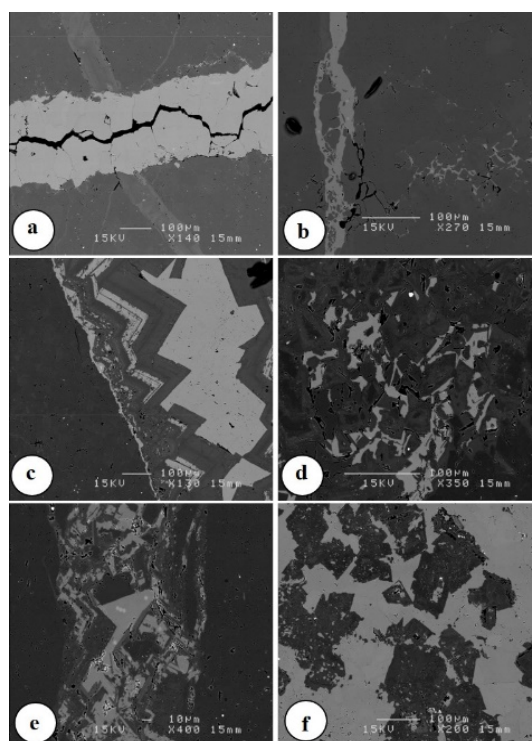
Fig. 3. by Scanning Electron Microscope backscattered images of Kharus Formation. a) Two stages of dolomite generation are FDD and vein-filling dolomites and later stage fracture-filling calcite cement. b) Filling of fractures and intercrystalline porosity by calcite cement. c & e) Fracture filling by cyclic dolomite and calcite cements. d) Cementation of intercrystalline porosity by calcite. f) Dedolomitization stage, where the pervasive dolomite crystals undergo replacement by calcite.

The third unit is a dark grey six-meter-thick stromatolitic dolomite, which is fine-medium crystalline and crosscut by microfractures cemented by dolomite spars. The fourth and fifth units are coarse crystalline dolomite units with a total thickness of 4 meters and are crosscut by both micro and macro fractures cemented by dolomite crystals. Unit six is 4 meters thick and composed of light grey microcrystalline dolomite. Rhombic dolomite and coarse calcite spars are found as cementing crystals within the fractures. Unit seven is a 5-meter-thick massive medium crystalline dolomite, which is crosscut by several fractures cemented by dolomite, calcite, and iron oxides. Unit 8 is a thinly laminated 10-meter-thick dolostone. The layers within unit 8 are either composed of fine cloudy dolomite crystals or medium dolomite crystals. The fractures found in this unit are cemented by dolomite and calcite spars. The younger (top) unit of the exposed section of the Kharus Formation is 2-meter-thick massive dolomite that is coarse crystalline and intercalated by several dolomite fractures.

Backscattered images by the SEM for the top of the Kharus Formation (Cambrian) reveal the existence of calcite spars as fracture filling crystals and intercrystalline porosity cement within the dolomites (Figure 3). In addition, the Backscattered images revealed the presence of zoned rhombic dolomite crystals, which contain alternating zones of calcite and dolomite. Furthermore, backscattered images show the presence of heavy minerals (Figure 3).

Trace element compositions of calcite and dolomite crystals and the crosscutting relationship between the different texture components were revealed by studying the thin polished sections with a Cathodoluminescence microscope. The zoned cathodoluminescence patterns in the crystals, especially void-filling crystals, typically denote fluctuations in Mn and Fe values. Further, the rock-forming crystals show differences in the luminescence colors, which signify the interplay of various crystallization stages with time. Cathodoluminescence images are a good indicator of the different fabric components of any rock. The exposed section of the Kharus Formation texture components is shown in (Figure 4) as inferred from the cathodoluminescence images.
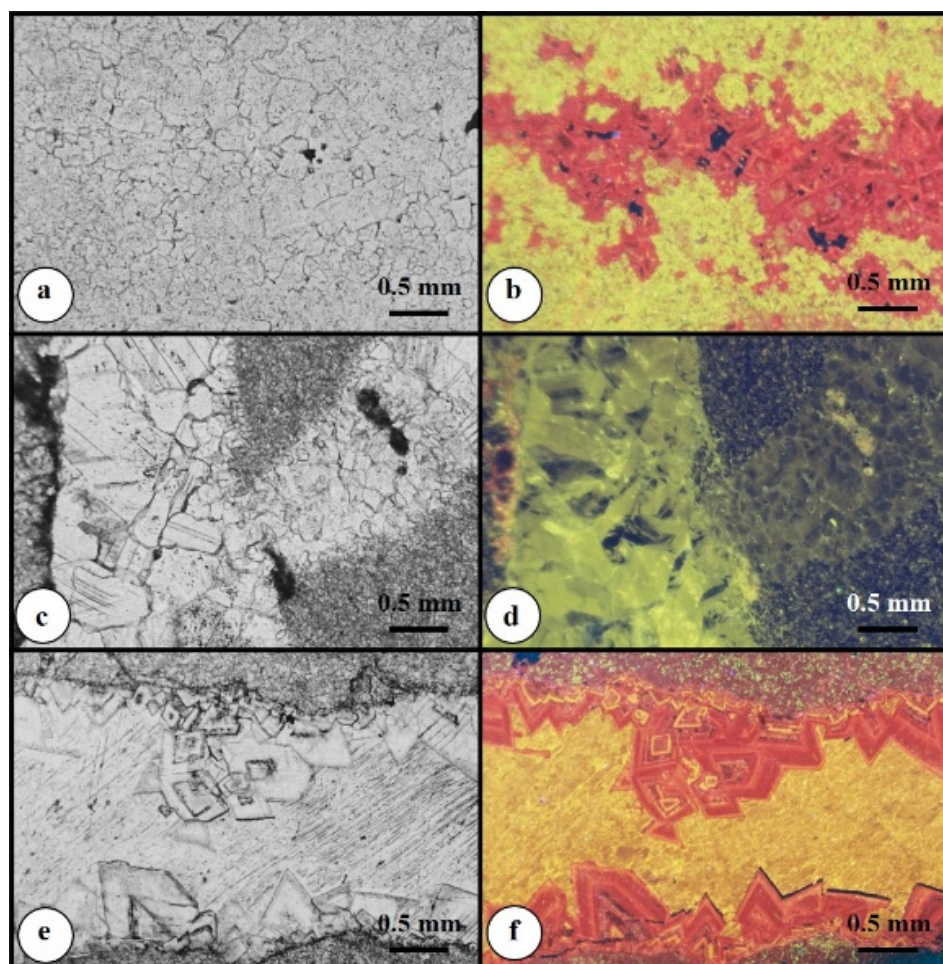
Fig. 4. Cathodoluminescence and polarizing microscope photomicrographs of texture components within the uppermost section of the Kharus Formation. a) Photomicrograph taken under plane-polarized light (ppl) of a polycrystalline dolomite sample composed of clear planar fine to medium dolomite crystals. b) Cathodoluminescence photomicrograph showing the same view as in (a); First stage dolomite (yellow luminescence), aggraded dolomite crystals (red luminescence). c) Photomicrograph taken under ppl of the oldest exposed unit from the Kharus Formation, which is a limestone unit affected by fracturing that is cemented by calcite and dolomite. d) Cathodoluminescence photomicrograph showing the same view as in (c); Rock-forming calcite (dark grey luminescence), calcite cementing crystals (yellowish-green), and dolomite cementing crystals (dark green). e) Photomicrograph taken under ppl of a microcrystalline dolomite sample, showing different stages of fracture-filling calcite and dolomite crystals. f) Cathodoluminescence photomicrograph showing the same view as in (e); microcrystalline dolomite (dark grey luminescence) and fracture-filling calcite (yellow luminescence) and rhombic zoned dolomite (alternating bands of red-yellow-dark grey luminescence).

The Permian-Triassic dolomites exhibit rocks displaying both fabric-preserving dolomitization (FPD) and fabric-destroying dolomitization (FDD) textures (Figure 5). The inferred precursor limestones that experienced dolomitization include stromatolites, mudstones, intraformational breccias, wackestones, packstones, grain/packstone, and grainstones (Al-langawi 2006). The rocks are mainly deposited in intertidal zones, supratidal zones, shoals, tidal bars, reefs, and back-reefs (Al-langawi 2006).
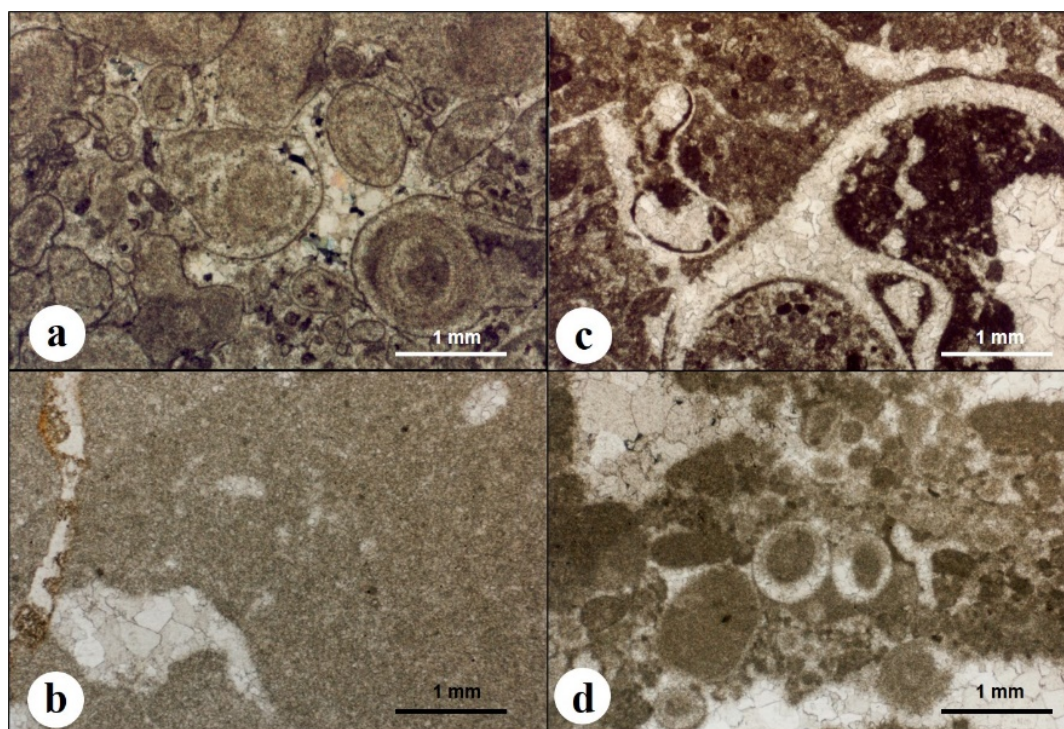
Fig. 5. Photomicrographs taken under plane-polarized light from samples of the Permian-Triassic dolomites. a) FPD of a grainstone. b) FPD of a mudstone. c) FPD of a bioclastic peloidal wackestone. d) FPD of a peloidal-oolitic packstone.

The study of the Palaeozoic-Mesozoic rock samples from all locations indicates that dolomitization is not restricted to a particular depositional environment. Nonetheless, field observations and the petrographic study revealed no evidence related to evaporates within the dolomites and limestones.

4. Geochemistry

Geochemical investigations on whole-rock samples displaying different degrees of preservation reveal a general slight Ca enrichment within rocks that experience FPD and near to stoichiometric compositions for the crystalline dolostones (Al-langawi 2006). Further, whole-rock analyses on Permian-Triassic dolomites indicate low concentrations of Fe, Mn, and Sr, which is evidence for near-surface dolomitization (Al-langawi 2006). Whole-rock analyses on pre-Permian dolomites indicate elevated concentrations of iron and low concentrations of strontium. Zhang *et al*. 2004, showed that high Mn and Fe combined with low Sr concentrations are associated with deep flowing hydrothermal fluids, whereas high Sr, moderate Fe, and low Ba and Mn are possible due to dolomitizing fluids late burial.

The microprobe quantitative analysis showed no systematic differences in Ca, Mg, Mn, and Fe concentrations within rock-forming dolomite crystals. Nonetheless, probe analysis on void-filling sparry dolomites revealed fluctuating fluid chemistry during crystallization which is reflected in Fe and Mn concentration (Figure 6).
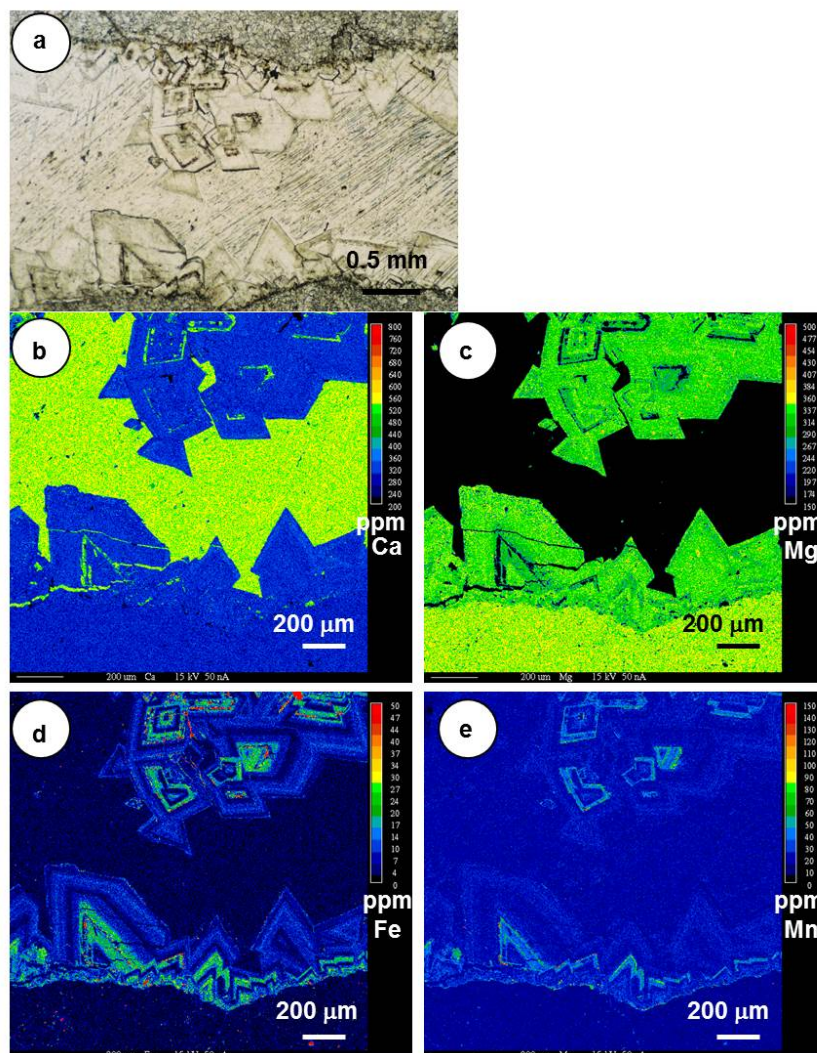
Fig. 6. Microprobe photomicrographs showing the distribution and concentration of the major and trace elements in one of the samples from the top part of the Kharus Formation-concentration (ppm).

Oxygen $\delta^{18}O$ and carbon $\delta^{13}C$ isotope analyses are conducted on samples with a range of textural and compositional variations (Table 1 and Figure 7). The dolomite crystals have $\delta^{18}O$ values ranging from +0.7 to -7.91 ‰ PDB (average of -3.00 ‰) and $\delta^{13}C$ values ranging from +5.86 to -0.7 ‰ PDB (average of +3.06 ‰). Plotting $\delta^{18}O$ against $\delta^{13}C$ for the chosen samples reveals that dolomites fall within two distinctive sections. The microcrystalline, fine, and medium dolomite crystals include nearly constant values of $\delta^{18}O$ and $\delta^{13}C$. Figure 7 shows that dolomites that are constituted of coarse to very coarse crystals are depleted in $\delta^{18}O$ compared to dolomites that are made of finer crystal sizes (Al-langawi 2006). Figure 7 was constructed to infer a possible origin of the Palaeozoic-Mesozoic Oman Mountain dolomites compared to various published data. The dolomites from the Oman Mountains do not fall within the region indicated by Slater (2007) for hydrothermal dolomitization of the Lower Palaeozoic dolomite reservoirs of the Mohawak Valley suggested for host rock and dolomite cement. None of the dolomites correlate to compositions inferred by Choquette & Steinen (1980) as the mixed-water origin and by Perkins *et al*. (1994) as the sabkha origin.

Table 1. Oxygen ($\delta^{18}O$) and carbon ($\delta^{13}C$) isotope data for the Palaeozoic-Mesozoic dolomites from different locations throughout the Oman Mountains.

Sample No.	$\delta^{18}O$	$\delta^{13}C$
Microcrystalline Dolomite		
Bih Formation 8-1	-1.98	1.41
Ghail Formation 3	-1.66	3.1
Hagil Formation 29-1	-3.44	2.73
Hagil Formation 6	-1.06	3.1
Mahil Formation 6-2	-1.11	1.42
Milaha Formation 50	-1.18	0.03
Saiq Formation 13-2	-3.42	4.94
Fine-Medium Crystalline Dolomite		
Bih Formation 16	-3.74	1.61
Bih Formation 5	-4.58	1.76
Bih Formation 8-2	-2.43	1.01
Kharus Formation 1	-0.37	4.39
Mahil Formation 2	-1.01	0.07
Maqam Formation 10-1	-1.94	5.43
Maqam Formation 10-2	-1.14	5.55
Maqam Formation 5	-3.31	5.57
Milaha Formation 54	-1.32	-0.7
Saiq Formation 17-1	0.7	4.14
Saiq Formation 17-2	-2.6	4.69
Saiq Formation 18	-2.74	4.7
Saiq Formation 7-1	-4.12	5.86
Saiq Formation 7-2	-3.5	1.66
Saiq Formation 8	-0.21	4.86
Saiq Formation 9	0	5.51
Coarse Crystalline Dolomite		
Ghail Formation 46	-7.91	3.28
Hagil Formation 29-2	-6.25	2.74
Kharus Formation 13-1	-5.31	4.7
Mahil Formation 6-1	-5.92	1.63
Maqam Formation 10-3	-6.15	3.31
Maqam Formation 14	-6.43	3.18
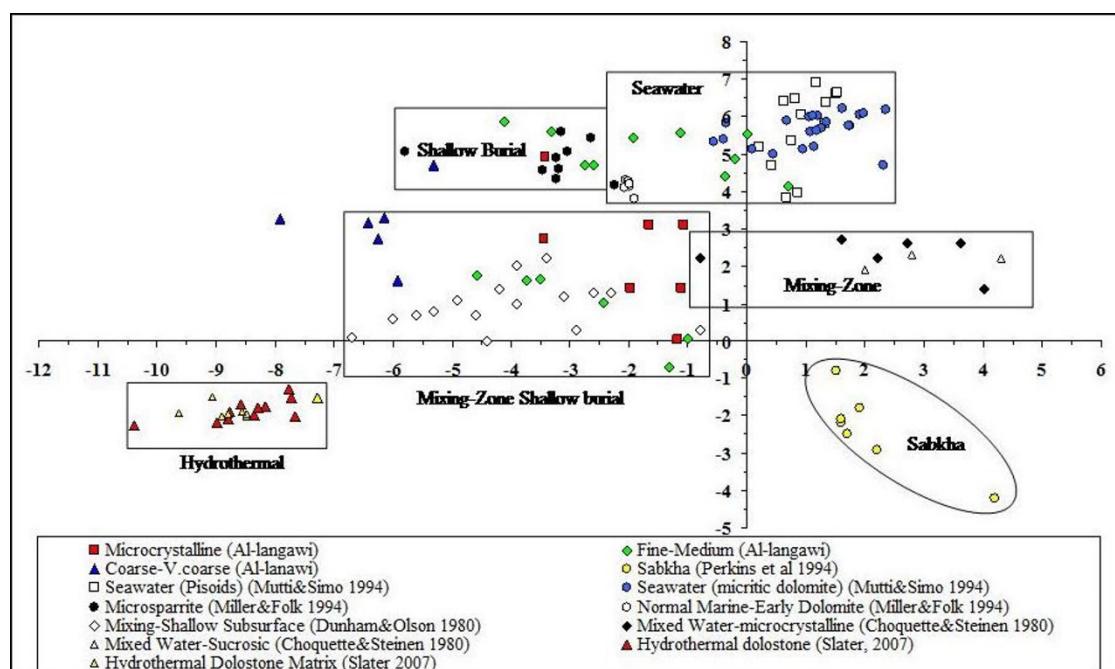
Fig. 7. Comparison of the isotopic data of the Palaeozoic-Mesozoic Oman Mountain dolomites with other inferred dolomitization mechanisms (Modified after Al-langawi, 2006).

The isotope values strongly suggest that host rocks were replaced by microcrystalline and medium crystalline dolomites in shallow burial environments by modified seawater at a formation temperature of ≤ 60°C (Miller & Folk 1994). Figure 7 suggests early dolomitization by normal marine waters (Mutti & Simo 1994; Miller & Folk 1994). Huang *et al*. 2014, noted that low dolomitization formation temperature produces FPD. They also indicated that formation temperature is generally higher for dolomite cement than for replacive dolomites. Warren 2000 postulated that $\delta^{18}O$ values between +1 and +5 ‰ PDB indicate marine water dolomitization. Al-langawi 2006, suggested that the coarse and very coarse crystalline dolomites and baroque dolomites may have formed under shallow burial settings marked by increases in temperature. Figure 7 reveals that some microcrystalline, fine, and medium crystalline dolomite samples fall within the field of mixed-water dolomites displayed by Dunham & Olson (1980).

5. Discussion

There are several essential aspects to take into consideration when studying the dolomitization of a given rock succession, which are essential in the inference of dolomitization processes and the construction of suitable dolomitization models (Al-langawi 2006). These aspects consist of: 1- Original environment of deposition, 2- Palaeogeographic setting, 3- Stratigraphic relationships with adjacent formations, 4- Petrography, 5- Stoichiometry and the degree of ordering in the dolomites, 6- Trace element concentrations and stable isotope distributions. In the case of the pre-Permian to Triassic dolomites, different paragenetic phases occurred that indicate fluctuations in sea level and hence, fluctuations in the environment of dolomitization (marine, meteoric, and mixing zone phreatic environments). The main factor controlling the type and degree of dolomitization that the original limestone underwent was the transferal in the phreatic zones. The primary stage of cementation that host rocks experienced before or

during dolomitization governs the dolomitization changes (Al-langawi 2006). The study revealed that some Triassic rocks retained their original composition as limestones, but some were affected by patchy replacement by dolomite crystals. Figure 8 is constructed to clarify and understand the different paragenetic phases that affected the Palaeozoic-Mesozoic rocks. Micritization of bioclasts was the first diagenetic stage that affected the precipitated allochems and formed micritic rims around the bioclasts (Figure 8). Later, five diagenesis phases occurred due to the fluctuation in the phreatic zone after burial. Most Palaeozoic-Mesozoic carbonates experienced diagenesis as explained in phase 1, and fewer samples displayed diagenetic development as explained in phases 2 and 3 (Figure 8, Table 2).

Table 2. Inferred Diagenetic Phases for the Palaeozoic-Mesozoic dolomites from Oman Mountains.

Phase 1	Phase 2	Phase 3	Phase 4	Phase 5
1. Under seawater conditions and shortly after deposition the micrite comprising all the allochems was replaced by FPD, and nearly equicrystalline fine cloudy nonplanar dolomite crystals replaced the internal structure of bioclasts.	1. Cementation of the lime sediments by either high-Mg calcite or aragonite isopachous crystals on the seafloor.	1. Dissolution of aragonitic allochems, especially the bioclasts after the development of micritic envelops.	1. Minor compaction of the fragile micritic envelopes and the isopachous cement around the bioclasts.	Fabric destroying dolomitization. The rapid replacement of limestones and several stages of dissolution and re-precipitation of dolomite crystals produced rocks exhibiting crystalline textures. The rocks developed after limestones and dolomites that were created under any of the Phases (1-4).
2. Cementation by Clear prismatic and drusy isopachous dolomite crystals around the outer surfaces of allochems including the bioclasts.	2. Replacement of the original allochems and micrite matrix by FPD, mimetic dolomitization of the isopachous cement by cloudy crystals, and replacement of the bioclasts by fine cloudy nonplanar dolomite crystals.	2. Precipitation of isopachous low-Mg calcite cement around the outer and inner surfaces of the biomoulds.	2. Some rocks underwent marine water diagenesis as in (stage 1- Phase 1) and (stage 2- Phase 2).	
3. The stromatolites and mudrocks underwent FPD by microcrystalline cloudy dolomites under the same marine water conditions, which preserved the original structures of the rocks. During this stage microcrystalline and fine nonplanar dolomite crystals mimicked the ooids within packstones and grainstones, and replacement of the geopetal sediment within fenestrae.	3. Then, the rocks experienced the same diagenetic stages as described in (stages 3-6 from Phase 1).	3. Minor compaction of the fragile micritic envelopes and the isopachous cement around the bioclasts.	3. Dissolution of the aragonitic components, especially bioclasts and aragonitic cortices within ooids due to decrease in sea level	
4. Further blocking of the primary porosities by fine to medium nonplanar dolomite crystals.		4. Cementation of the intergranular, intragranular and mouldic porosity by sparry calcite mosaics, but without complete blocking of the pore spaces.	4. Cementation of the intragranular porosity by dolomites crystals which are clear, planar and nonplanar, showing different luminescence from that of the microcrystalline dolomites and comparable to that of the second dolomite cement generation found in the leftover voids after (stage 1- Phase 1).	
5. Cementation of vugs, fractures and larger intergranular cavities by dolomites showing textures and luminescence different from those of the replacive dolomites and fine-medium nonplanar dolomite cement (stages 1-4). The dolomite crystals are zoned and either started as clear rhombic isopachous crystals and progressed into planar-e coarser drusy sparry cement or had planar-s texture that also shows competitive growth towards cavity centres.		5. Cloudy dolomite crystals mimetically replaced the original allochems, the isopachous meteoric cement, and the sparry calcite cement soon after stage 4.	5. The rocks then followed the same diagenetic stages described for Phase 1 (stage 2-6).	
6. Aggradation (neomorphism) of the host dolomites formed under stages (1-5) to slightly coarser nonplanar and sometimes planar cloudy crystals or crystals with cloudy centres and clear rims, which are nearly equicrystalline.		6. Competitive growth within cavities by clear dolomite overgrowths and clear sparry dolomite cement.		
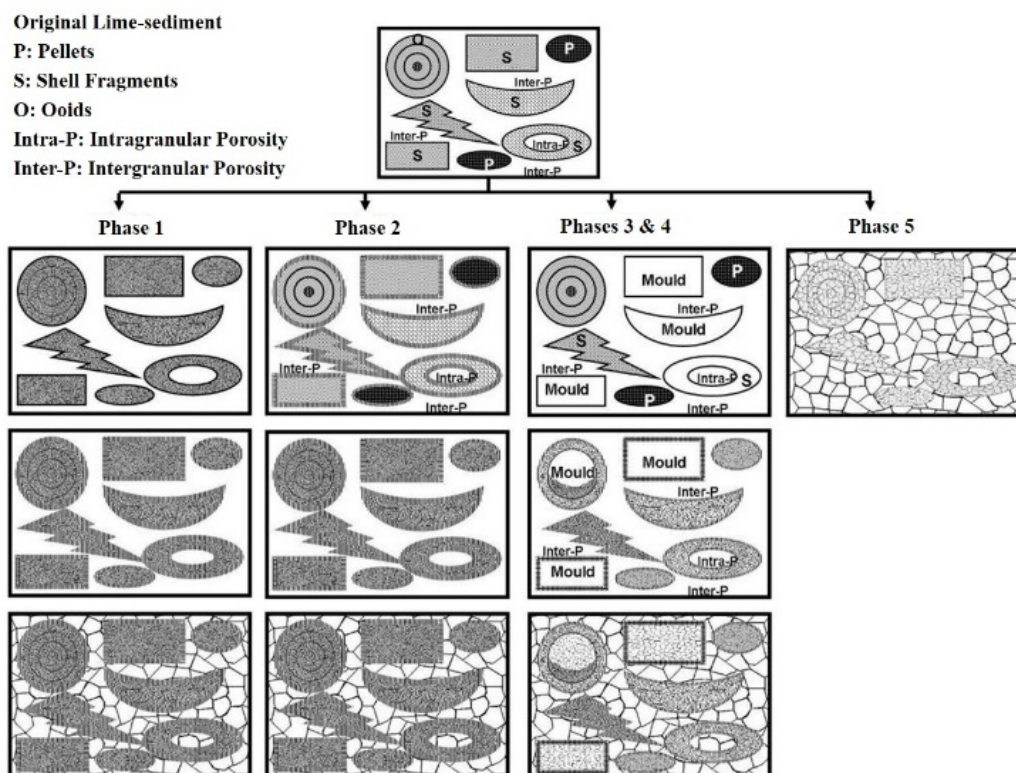
Fig. 8. Proposed major Digenetic Phases for the Palaeozoic-Early Mesozoic carbonates-Oman Mountains.

Diagenetic Phase 1: produced dolomitic rocks that show perfect and near-perfect preservation of the initial host rock textural components (Table 2). Comparable luminescence patterns gave clear evidence indicating a similar environment of dolomitization, which is the development under the same marine fluid settings with a slight change in water chemistry during stages 1-4. The zoned luminescence patterns in dolomite developed during stage 5 strongly suggest changes in the dolomitizing fluid chemistry than the fluids led to stags 1-4. Table 2 shows that the last stage in FPD development is the aggrading of crystals formed during stage 3. The luminescence patterns for the aggraded dolomite crystals strongly suggest that the aggradation was initiated simultaneously as in stage 3, but further aggradation was under the same fluid conditions as in stage 5.

Diagenetic Phase 2: also produced dolomitic rocks that show perfect and near-perfect conservation of the primary fabric components. Table 2 shows either high-Mg calcite or aragonite isopachous cement that occurred on the seafloor before the dolomitization stages. The same dolomites formed during stage 1 (Diagenetic Phase 1) replaced the primary high-Mg and isopachous calcite and aragonite cement. Later dolomitization progressed as described in stages 3-6 in the diagenetic phase 1.

Diagenetic Phase 3: also produced dolomitic rocks that show perfect and near-perfect preservation of the original host rock fabric components. A petrographic study indicates that the rocks underwent a dissolution stage which led to the dissolution of aragonitic components of the host limestone. Then a compaction stage post precipitation of isopachous low-Mg calcite cement surrounding the outer and inner boundaries of the biomoulds. Petrographic and

13

luminescence patterns strongly suggest that dolomitization of these host rocks started by replacing the previously formed calcite cement and allochems and ended by cementation of the leftover porosities by clear dolomite mosaics (Table 2).

Diagenetic Phase 4: also produced dolomitic rocks that show perfect and near-perfect preservation of the original host rock fabric components. The dolomitization was not preceded by calcite cementation. The diagenesis started soon after precipitation under marine water conditions (Table 2). The evidence for the meteoric water digenesis is exhibited by the dissolution of aragonitic bioclasts and ooid grains. Luminescence patterns strongly suggest that dolomites formed under stage 3 formed under different water chemistry than first stage dolomitization.

Diagenetic Phase 5: produced dolomitic rocks that show complete obliteration of the original rocks fabric components (FDD). But few rocks comprise a limited number of relicts which aided some interpretation. The dolomites that show crystalline texture and destruction of the original host rock fabric could have undergone any of the four diagenetic phases previously described.

All the above-mentioned diagenetic phases ended by cementation of fractures and leftover intercrystalline porosity by either baroque dolomite or calcite, and some are affected by patchy dedolomitization (Figures 3 and 4).

6. Conclusions

Petrographic evidence in relation to the deferent diagenetic phases, combined with the geochemical results, clearly indicates that the Permian-Triassic Oman Mountain carbonates have developed mainly according to what is described in diagenetic phases 1-4. This kind of diagenesis produced dolomites that retained their host limestone textures and fabrics and relics of their components. This implies that dolomitization was under marine conditions soon after the deposition of the host carbonate sediments and continued according to the shift and fluctuation in the phreatic environment.

Some of the Permian- Triassic rock samples and the top 36 meters of Kharus Formation (Cambrian) underwent diagenesis as described in diagenetic phase 5. The dolomites, in this case, show complete obliteration of the host limestones by crystalline dolomites; hence no evidence of any texture or fabrics exists. Geochemical data support the diagenesis under shallow burial to slightly thermal conditions for the Cambrian Kharus Formation and some Permian-Triassic dolomites.

The results generally suggest early dolomitization by normal seawater, modified marine waters with increased temperature, and relatively warm marine water settings in the shallow subsurface. Evidence of seawater and shallow burial dolomitization include micritization, cementation by isopachous prismatic and drusy dolomite crystals, and fine-medium nonplanar dolomite cement, planar-e coarse drusy dolomite cement, and replacement by fabric-preserving dolomitization (fine-medium cloudy nonplanar dolomite). The replacement of first stage dolomites, the replacement of medium to coarse planar dolomite crystal fabric-destroying dolomitization, and cementation by baroque dolomite are evidence of relatively warm marine water diagenesis in the shallow subsurface. Selective dissolution of aragonitic bioclasts and

partial dissolution of the cortices of some ooids due to meteoric water are clear evidence of meteoric phreatic zone diagenesis before dolomitization.

Geochemical evidence, especially Ca/Mg ratios within dolomite crystals and isotope data, are comparable to the diagenetic phases that affected the Oman Mountain rocks. The differences in saturation, oxidation, and pH of the dolomitizing fluids are signified by Fe and Mn concentrations fluctuations. Such as, Moderate to low Na values, low Fe content, and depleted ^{18}O values indicate the formation of these dolomites at temperatures ranging between 20-60°C and oxidizing meteoric dolomitizing fluids. In addition, High Al and Si concentrations due to fast nucleation led to the incorporation of these elements as inclusions within the crystals, and low Fe concentrations and lack of related minerals, such as pyrite within the dolomites reflect oxidizing conditions, all are evidence of marine fluid diagenesis.

The dolomitization of the Palaeozoic-Mesozoic carbonates implies the involvement of substantial amounts of fluids containing Mg. This dolomitization was continuous, and adequate time was available.

ACKNOWLEDGMENTS

References

Adams, A.E, MacKenzie, W.S, and Guilford, C. (1984). Atlas of sedimentary rocks under the microscope. Longman Group Limited, England.

Al-langawi, A.J. (2006). Fabric preserving and fabric destroying dolomitization: A case of seawater dolomitization. SQU Journal for Science, Sultan Qaboos University 11: 39-67.

Arenas, C., Alonso Zarza, A. M., and Pardo, G. (1999). Dedolomitization and other early diagenetic processes in Miocene Lacustrine deposits, Ebro Basin (Spain). Sedimentary Geology 125: 23-45.

Baud, A. and Richoz, S. (2013). Permian-Triassic Transition and the Saiq/Mahail boundary in the Oman Mountains: Proposed correction for lithostratigraphic nomenclature. GeoArabia 18: 87-98.

Choquette, P.W. and Steinen, R. P. (1980). Mississippian non-supratidal dolomite, Ste.Genevieve limestone, Illinois Basin: evidence for mixed-water dolomitization. In: Zenger D.H., and Dunham J.B., (eds.) Concepts and Models of Dolomitization. SEPM Spec.Publ, 28, pp 163-196.

Coleman, R.G. (1981). Tectonic setting for ophiolite obduction in Oman. Journal of Geophysical Research 86(B4): 2497-2508.

Dawson, W., C., and Carozzi, A. V. (1993). Experimental deep burial, fabric-selective dissolution in Pennsylvanian Phylloid Algal Limestones. Carbonates and Evaporites, 8(1): 71-81.

Dunham, J.B. and Olson, E.R. (1980). Shallow subsurface dolomitization of subtidally deposited carbonate sediments in the Hanson Creek Formation (Ordovician-Sillurian) of Central Nevada. In: Zenger D.H., and Dunham J.B., (eds.) Concepts and Models of Dolomitization. SEPM Spec. Publ, 28: 39-162.

Gealey, W.K. (1977). Ophiolite obduction and geologic evolution of the Oman Mountains and adjacent areas. Geological Society of America Bulletin 88:1183-1191.

Glennie, K.W., Boeuf, M.G.A., Hughes Clark, M.W., Moody-Stuart, M., Pilaar, W.F.H., and Rienhardt, B.M. (1973). Late cretaceous nappes in the Oman Mountains and their geologic significance. The American Association of Petroleum Geologists Bulletin 57:5-27.

Glennie, K.W., Boeuf, M.G.A., Hughes Clark, M.W., Moody-Stuart, M., Pilaar, W.F.H., and Rienhardt, B.M. (1974). The geology of the Oman Mountains. Verhandelingen Van Hert Koninklijik Nederlands geologisch minjbouwkunding Genoostschap 31(1 and 2):423 pp.

Glennie, K.W., Hughes Clark, M.W., Boeuf, M.G.A, Pilaar, W.F.H., and Reinhardt, B.M. (1990). Inter-relationship of Makran-Oman Mountains belts of convergence. In: Robertson A.H.F., Searle M.P., and Ries A.C., (eds.) The geology and tectonics of the Oman region, Geological Society Special Publ., 49, pp 773-786.

Gunatilaka, H. A. (1987). The dolomite problem in the light of recent studies. Modern Geology 11: 311-324.

Huang, S., Huang, K., LÜ, J., and Lan, Y. (2014). The relationship between dolomite textures and their formation temperature: a case study from the Permian-Triassic of the Sichuan Basin and the Lower Paleozoic of the Tarim Basin. Petroleum Science 11(1):29-51.

Khalaf, F. and Al-Zamel, A. (2018). Occurrence of recent dedolomite crust on pedogenetic calcrete in Al-Jabal Al-Akhdar, northern Oman. Kuwait Journal of Science 45(1): 128-137.

McKenzie, J. A., Hsu, K. J., and Schneider, J. F. (1980). Movement of subsurface waters under the sabkha, Abu Dhabi, U.A.E., and its relation to evaporative dolomite genesis. In: Zenger, D. H., Dunham, J. B., and Ethington, R. L. (eds.), Concepts and Models of Dolomitization, Society of Economic Palaeontologists and Mineralogists, Special Publ. 28: 11-30.

Mann, A., and Hanna, S.S. (1990). The tectonics evolution of pre-Permian rocks, Central and Southeastern Oman Mountains. In: Robertson A.H.F., Searle M.P., and Ries A.C., (eds.) The geology and tectonics of the Oman region. Geological Society Special Publ., 49: 27-37.

Mattes, B. W., and Mountjoy, E. W. (1980). Burial dolomitization of the Upper Devonian Mette Buildup, Jasper National Park, Alberta. In: Zenger, D. H, Dunham, J. B., and Ethington, R. L. (eds.), Concepts and Models of Dolomitization, Society of Economic Palaeontologists and Mineralogists, Special Publ. 28: 259-297.

Miller, J.K. and Folk, R.L. (1994). Petrographic, geochemical and structural constraints on the timing and distribution of postlithification dolomite in the Rhaetian Portoro ('Calcar Nero') of the Portovenere Area, La Spezia, Italy. In: Purser B.H., Tucker M.E., and Zenger D.H., (eds.) Dolomites: A Volume in Honour of Dolomieu, International Association of Sedimentologists Special Publ. 21: 187-202.

Murris, R.J. (1980). Middle East: Stratigraphic evolution and oil habitat. American Association of Petroleum Geologists Bulletin 64(5):567-618.

Mutti, M. and Simo, J.A. (1994). Distribution, petrography, and geochemistry of early dolomite in cyclic shelf facies, Yates Formation (Guadalupian), Capitan Reef Complex, USA. In: Purser B.H., Tucker M.E., and Zenger D.H., (eds.) Dolomites: A Volume in Honour of Dolomieu, International Association of Sedimentologists Special Publ. 21, pp 91-109.

Perkins, R.D., Dwyer, G.S., Rosoff, D.B., Fuller, J., Baker, P.A., and Lloyd, R.M. (1994). Salina sedimentation and diagenesis: West Caicos Island, British West Indies. In: Purser B.H., Tucker M.E., and Zenger D.H., (eds.) Dolomites: A Volume in Honour of Dolomieu, International Association of Sedimentologists Special Publ. 21, pp 37-54.

Randazzo, A. F., and Cook, D. J. (1987). Characterization of dolomitic rocks from the coastal mixing zone of the Floridan aquifer, Florida. U.S.A. Sedimentary Geology 59: 269-277.

Ricateau, R. and Riche, P.H. (1980). Geology of the Musandam Peninsula (Sultanate of Oman) and its surroundings. Journal of Petroleum Geology 3(2):139-152.
Robertson, A.H.F., Blome, C.D., Cooper, D.W.J., Kamp, A.E.S., and Searle, M.P. (1990). Evolution of the Arabian continental margin in the Dibba Zone, Northern Oman Mountains. In: Robertson A.H.F., Searle M.P., and Ries A.C., (eds.) The geology and tectonics of the Oman region. Geological Society Special Publ., 49, pp 251-286.

Searle, M.P. and Graham, G.M. (1982). "Oman Exotics"-Oceanic carbonate buildups associated with the early stages of continental rifting. Geology 10:43-49.

Searle, M.P., James, N.P., Calon, T.J., and Smewing, J.D. (1983). Sedimentological and structural evolution of the Arabian continental margin in the Musandam Mountains and Dibba zone, United Arab Emirates. Geological Society of America Bulletin 94:1381-1400.

Slater, B.E. (2007). Outcrop Analog for Lower Paleozoic hydrothermal dolomite reservoirs, Mohawk Valley. NY. Master's degree Thesis, University at Albany, State University of New York.

Tucker, M.E. (2001). Sedimentary Petrology: An introduction to the Origin of Sedimentary Rocks. Third Edition. Blackwell Publishing company, U.S.A., U.k., Australia.

Veerle, V. and Cedric, J.M. (2012). Influence of climate and dolomite composition on dedolomitization: Insights from a multi-proxy study in the Central Oman Mountains. Journal of Sedimentary Research 82(3-4):177-195.

Warren, J. (2000). Dolomite: Occurrence, evolution and economically important Associations. Earth-Science Reviews 52 (1-3):1 – 81.

Welland, M.J.P. and Mitchell, A.H.G. (1977). Emplacement of the Oman Ophiolite: A mechanism related to subduction and collision. Geological Society of America Bulletin 88:1081-1088.

Wilson, H.H. (1969). Late Cretaceous eugeosynclinal sedimentation, gravity tectonics, and ophiolite emplacement in Oman Mountains, Southeast Arabia. The American Association of Petroleum Geologists Bulletin 53(3):626-671.

Wilson, A.O. (1985). Depositional and diagenetic facies in Jurassic Arab C and D reservoirs, Qatif field, Saudi Arabia. In: Roehl P.O., and Choquette P.W., (eds.) Carbonate petroleum reservoirs, Springer-Verlag, New York, pp 319-340.

Zainal Abidin, N.S., Raymond, R.R., and Bashah, N.S.I. (2017). Diagenetic history of late Oligocene-early Miocene carbonates in East Sabah, Malaysia. IOP Conf. Series: Earth and Environmental Science 88: 012016. doi: 10.1088/1755-1315/88/1/012016.

Zhang, W., Guan, P., Jian, X., Feng, F., and Zou, C. (2004). In situ geochemistry of Lower Plaleozoic dolomites in the northwestern Tarim Basin: Implications for the nature, origin, and evolution of diagenetic fluids. Geochemistry, Geophysics, Geosystems (G3) Journal 15(7):2744-2764. DOI: 10.1002/2013GC005194